Direct *ab initio* molecular dynamics study on a microsolvated S_N2 reaction of $OH^-(H_2O)$ with CH_3Cl

Hiroto Tachikawa[a)]
Division of Materials Chemistry, Graduate School of Engineering, Hokkaido University, Sapporo 060-8628, Japan

(Received 20 April 2006; accepted 23 June 2006; published online 5 October 2006)

Reaction dynamics for a microsolvated S_N2 reaction $OH^-(H_2O)+CH_3Cl$ have been investigated by means of the direct *ab initio* molecular dynamics method. The relative center-of-mass collision energies were chosen as 10, 15, and 25 kcal/mol. Three reaction channels were found as products. These are (1) a channel leading to complete dissociation (the products are $CH_3OH+Cl^-+H_2O$: denoted by channel I), (2) a solvation channel (the products are $Cl^-(H_2O)+CH_3OH$: channel II), and (3) a complex formation channel (the products are $CH_3OH\cdots H_2O+Cl^-$: channel III). The branching ratios for the three channels were drastically changed as a function of center-of-mass collision energy. The ratio of complete dissociation channel (channel I) increased with increasing collision energy, whereas that of channel III decreased. The solvation channel (channel II) was minor at all collision energies. The selectivity of the reaction channels and the mechanism are discussed on the basis of the theoretical results. © *2006 American Institute of Physics*. [DOI: 10.1063/1.2229208]

I. INTRODUCTION

Bimolecular nucleophilic substitution (S_N2) reactions in the gas phase have been investigated extensively from the theoretical and experimental points of view due to their central importance in recent organic chemistry.[1–3] From the theoretical points of view, *ab initio*, classical, and quantum chemical dynamics calculations[4–12] have been carried out by several groups. The energetics and potential energy surfaces (PESs) for the S_N2 reactions,

$$X^- + CH_3Y \rightarrow XCH_3 + Y^-(X,Y = F,Cl,Br,\text{and } OH), \quad (1)$$

were obtained by the *ab initio* method. The reaction rates for several systems were also investigated on the basis of transition state theory using the *ab initio* data. For the dynamics features, conclusive works on the reaction dynamics of the gas-phase S_N2 reactions have been carried out by Hase and co-workers.[13] They calculated classical trajectories on the analytical PES fitted to *ab initio* data and showed that the reaction proceeds via a direct mechanism in which there is no long-lived complex on the entrance or exit region. They also found that there are multiple mechanisms for these reactions. In the case of low collision energies, the reaction proceeds either via trapping in the precomplex region $X^-\cdots CH_3Y$, followed by non-Rice-Ramsperger-Kassel-Marcus (RRKM) dynamics or by a direct mechanism which is facilitated by C–Y stretch excitation. The reaction with high collision energy promotes a direct mechanism.

Recently, we have carried out direct *ab initio* molecular dynamics (MD) calculations[14] on S_N2 reactions expressed by

$$F^- + CH_3Cl \rightarrow CH_3F + Cl^-, \quad (2)$$

$$OH^- + CH_3Cl \rightarrow CH_3OH + Cl^-. \quad (3)$$

We found that the lifetimes of the complexes are short enough to proceed via a direct mechanism. Also, it was found for reaction (2) that the total available energy is partitioned into the relative translational mode between the products (43%) and the C–F stretching mode (57%) at zero collision energy. The other internal modes of CH_3F remain in the ground state. Also, the lifetime of the late complex is short. These features are in good agreement with previous dynamics studies by Hase and co-workers.[13]

From an experimental point of view, VanOrden *et al.*[15] measured the energy distribution of the products in the gas-phase S_N2 reaction (F^-+CH_3Cl) using Fourier transform ion cyclotron resonance (FT-ICR) spectroscopy, and found that the reaction proceeds with a large fraction of the exothermicity partitioned into the relative translational energy of the products.

Thus, many investigations on the gas-phase S_N2 reaction have been carried out from both theoretical and experimental points of view.[1–15] Nevertheless, fewer studies have addressed the role of solvation in these reactions.[16,17] From an experimental point of view, O'Hair *et al.* investigated solvent effects on the S_N2 reaction of fluoride ion with methyl chloride and measured the product ions formed by the reaction $F^-(H_2O)+CH_3Cl$.[18] They detected two ions, Cl^- and $Cl^-(H_2O)$, as products. This result has been interpreted to show that two reaction channels,

$$F^-(H_2O) + CH_3Cl \rightarrow CH_3F + Cl^- + H_2O \quad (4)$$

$$\rightarrow CH_3F + Cl^-(H_2O), \quad (5)$$

are observed with the microsolvated S_N2 reaction. Reaction (4) is a three-body dissociation (complete dissociation) in which all species are separated from each other. In reaction (5), the product chloride ion is solvated by a water molecule.

a)Electronic mail: hiroto@eng.hokudai.ac

They estimated that the branching ratio of reactions (4)/(5) is 3/1 (error bar is ±50%), although reaction (5) is more exothermic in energy than reaction (4). This is an interesting point in this reaction.

The energetics for the reaction $F^-(H_2O)+CH_3Cl$ were investigated by Hu and Truhlar using *ab initio* calculations.[19] The heats of reaction for channels I and II are calculated to be −2.0 and −17.4 kcal/mol at the MP2/aug-cc-pVTZ level of theory, respectively. We investigated reactions (4) and (5) by means of the direct *ab initio* MD method and concluded that reaction (5) becomes a minor channel because the hopping efficiency of H_2O from F^- to Cl^- is small in the collision.[20,21]

In 1995, Hierl *et al.*[22] used tandem mass spectroscopy to measure cross sections and product distributions for the S_N2 reaction $OH^-(H_2O)_n+CH_3Cl$ ($n=0-2$) over the relative collision energy range of 0.1–5.0 eV. They found that increasing the hydration number (n) decreases the S_N2 reaction probability. Collision-induced dissociation is the major process above 1.0 eV. At the low collision energy range, the reactions are expressed by

$$OH^-(H_2O)+CH_3Cl \rightarrow CH_3OH+Cl^-+H_2O \quad (6)$$

$$\rightarrow CH_3OH+Cl^-(H_2O). \quad (7)$$

Se and Morokuma calculated the energy diagram for this reaction.[23] However, the dynamic features of the reaction are unknown.

In the present study, direct *ab initio* MD calculations are applied to the microsolvated S_N2 reaction $OH^-(H_2O)+CH_3Cl$ in order to elucidate the reaction mechanism. The purposes of this study are to elucidate the origin of the preference for one reaction channel over the others and to elucidate the role of the solvent molecule in the reaction dynamics.

II. METHOD OF CALCULATION

The geometrical parameters for the collision system $OH^-(H_2O)+CH_3Cl$ are schematically illustrated in Fig. 1. The parameter r_1 indicates the intermolecular distance between the oxygen of OH^- and the carbon of CH_3Cl. The C–Cl bond distance of CH_3Cl is defined by r_2. In the reactive trajectory, r_1 decreases with increasing reaction time, whereas r_2 increases as a function of time. The parameter r_3 indicates the distance between Cl^- and H_2O. This parameter decreases in the case of the formation of $Cl^-(H_2O)$. The parameter r_4 indicates the oxygen-oxygen distance between OH^- and H_2O. The angle parameters α and ϕ mean angles of $CH_3Cl\cdots OH\cdots H_2O$ and H–C–H of CH_3Cl, respectively. It should be noted that collisions from backside ($\alpha=80°-180°$ and $\beta=0°-50°$) are assumed: $OH^-(H_2O)$ collides at the carbon atom of CH_3Cl. Also, a near zero impact parameter ($b\approx 0.0$ Å) was only considered in the present study. Hence, the product distribution obtained in the present calculation cannot be directly compared with experiments.

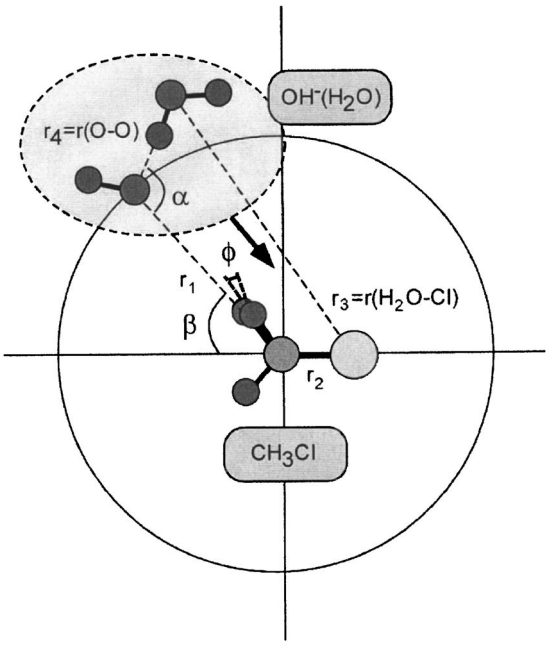

FIG. 1. Geometrical parameters for the reaction system $OH^-(H_2O)+CH_3Cl$.

The initial separation between $OH^-(H_2O)$ and CH_3Cl and the position of H_2O relative to $OH^-\cdots CH_3Cl$ (the angle of $H_2O-OH^-CH_3Cl$) were generated in the range $r_1=6.50-9.20$ Å and $\alpha=80°-180°$, respectively. At the start of the trajectory calculation, the velocities of the atoms of CH_3Cl were adjusted to give a temperature of 10 K as the classical vibrational distribution. The mean temperature of the system is defined by

$$T=\frac{1}{3kN}\left\langle \sum_i m_i v_i^2 \right\rangle, \quad (8)$$

where N is the number of atoms, v_i and m_i are the velocity and mass of the ith atom, and k is Boltzmann's constant. We choose 10 K as the simulation temperature. The velocities of atoms at the starting point were adjusted to the selected temperature. In order to keep a constant temperature of the system, a bath relaxation time (τ) was introduced in the calculation. We have chosen $\tau=0.01$ ps in all trajectory calculations.

In the case of collision dynamics, the collision energies at the initial separation were chosen as 10, 15, and 25 kcal/mol. The equations of motion for n atoms in the system are given by

$$\frac{dQ_j}{dt}=\frac{\partial H}{\partial P_j},$$

$$\frac{\partial P_j}{\partial t}=-\frac{\partial H}{\partial Q_j}=-\frac{\partial U}{\partial Q_j}, \quad (9)$$

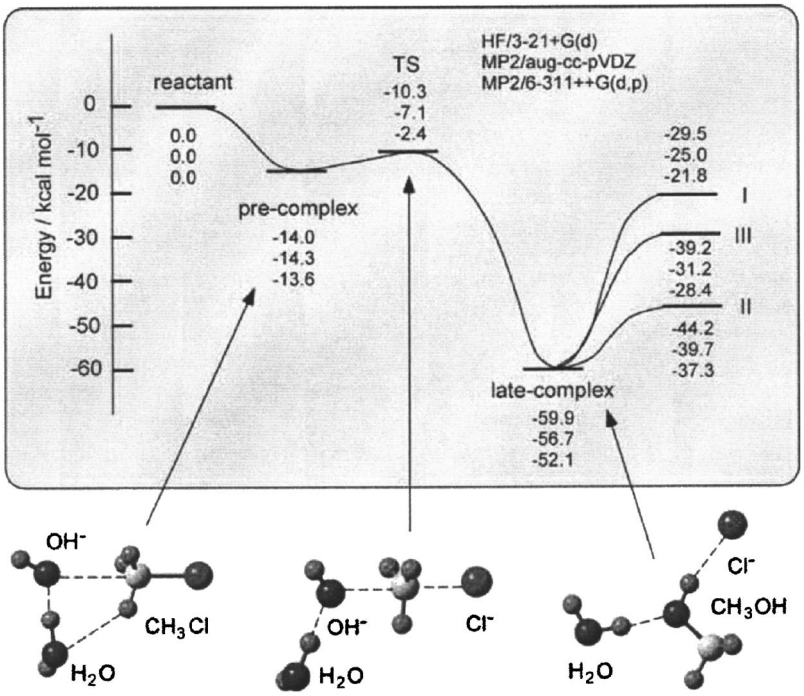

FIG. 2. Energy diagram for the reaction system $OH^-(H_2O)+CH_3Cl$ calculated at the HF/3-21+G(d), MP2/aug-cc-pVDZ, and MP2/6-311++G(d,p) levels of theory. The values mean the relative energies with respect to reactant (in kcal/mol). The products in channels I and II are ($CH_3OH+H_2O+Cl^-$) and ($Cl^-(H_2O)+CH_3OH$), respectively, while those in channel III are $CH_3OH-H_2O+Cl^-$. MP2/aug-cc-pVDZ values are cited from Ref. 23.

where $j=1-3N$, H is the classical Hamiltonian and Q_j, P_j, and U are the Cartesian coordinate of the jth mode, the conjugated momentum, and the potential energy of the system, respectively. These equations were numerically solved by the Runge-Kutta method. No symmetry restriction was applied to the calculation of the gradients. The time step size was chosen by 0.2 fs, and a total of 10 000 steps were calculated for each dynamics calculation. The drift of the total energy is confirmed to be less than 1×10^{-3}% throughout at all steps in the trajectory. The momentum of the center of mass and the angular momentum are assumed to zero.

In previous papers,[8] we showed that the HF/3-21+G(d) calculation gives a reasonable PES and dynamics features for the S_N2 reactions $F^-+CH_3Cl\rightarrow FCH_3+Cl^-$ and $OH^-+CH_3Cl\rightarrow CH_3OH+Cl^-$. Also, this level of theory gave a good result for the Cl^-+CH_3Cl reaction system.[13] Therefore, we used the 3-21+G(d) basis set in the direct *ab initio* MD calculation throughout. The HF/3-21+G(d) optimized geometries of CH_3Cl and $OH^-(H_2O)$ were chosen as initial structures. To obtain the structures and energetics for the reaction system, static *ab initio* calculations at the HF/3-21

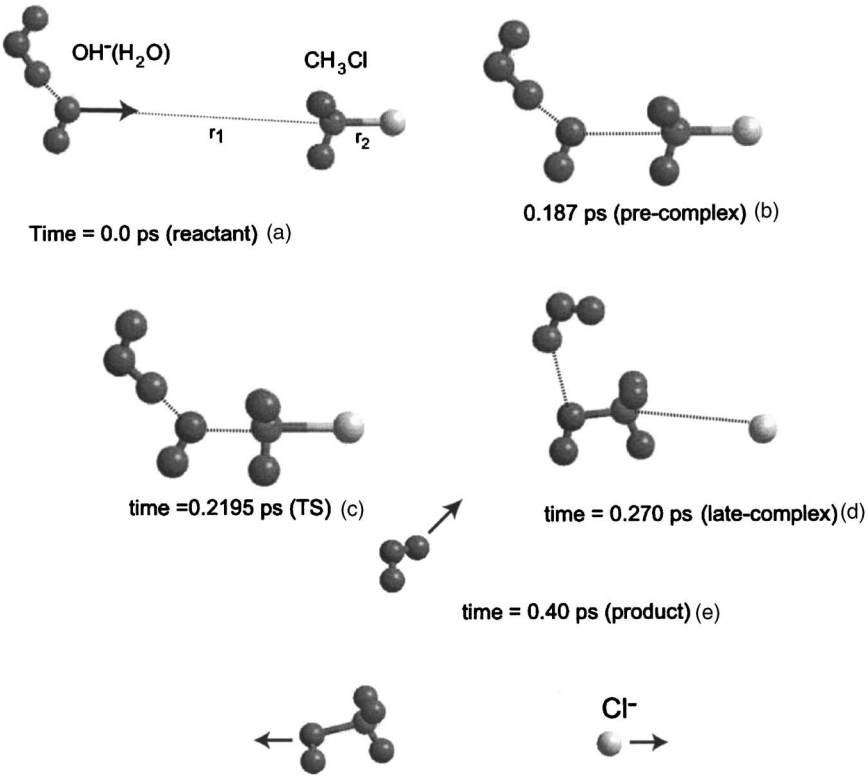

FIG. 3. Snapshots of the conformations for a typical trajectory for channel I illustrated as a function of reaction time.

+G(d), MP2/aug-cc-pVDZ, and MP2/6-311++G(d,p) levels[24] were carried out for the stationary points along the reaction coordinate.

III. RESULTS

A. Energetics

The reactant, intermediate complexes, transition state (TS), and product molecules are fully optimized at the HF/3-21+G(d), MP2/aug-cc-pVDZ, and MP2/6-311++G(d,p) levels of theory. We discuss the structures and energetics of the reaction system using the most sophisticated calculation,MP2/6-311++G(d,p). The potential energy diagram for the reaction is illustrated in Fig. 2. Zero level corresponds to the energy level of the reactant $OH^-(H_2O)+CH_3Cl$. It is found that a precomplex is first formed at the entrance region of the reaction, where the OH^- ion is trapped by a dipole moment of CH_3Cl. The water molecule binds to OH^- by a hydrogen bond. The distance of OH^- from $CH_3Cl(=r_1)$ and the bond length of C–Cl of $CH_3Cl(=r_2)$ are calculated to be 2.8197 and 1.8103 Å, respectively. Mulliken charges on OH^-, H_2O, and CH_3Cl are calculated to be −0.80, −0.14, and −0.06, respectively, indicating that almost all negative charges are localized on $OH^-(H_2O)$ (−0.94) in the precomplex. The $OH^-(H_2O)$ is trapped as a dipole bound state near CH_3Cl. The stabilization energy of the precomplex is calculated to be 13.6 kcal/mol relative to the reactant.

The energy level of the TS is lower in energy than that of the reactant (−2.4 kcal/mol), indicating that the S_N2 reaction has a negative activation energy. The distance of OH^- from $CH_3Cl(=r_1)$ is calculated to be 2.0620 Å, which is significantly shortened from that of the precomplex (r_1=2.8197 Å). The C–Cl bond length of $CH_3Cl(=r_2)$ is 2.1568 Å, which is greatly elongated (r_2=1.8103 Å for the precomplex). The charges on OH and Cl are calculated to be −0.69 and −0.43, respectively, indicating that half of the negative charges are transferred to the Cl atom of CH_3Cl at the TS. An imaginary frequency at the TS is calculated to be 592 cm^{-1}, which corresponds to the asymmetric stretching mode of $OH-CH_3-Cl$.

After the TS, a late complex is formed at the exit region of the reaction. In this complex, Cl^- is solvated by CH_3OH with a hydrogen bond, and H_2O is oriented toward CH_3OH. The charge on the Cl^- ion is −0.98, indicating that the negative charge is fully localized on the Cl^- ion. The stabilization energy of the late complex is calculated to be 52.1 kcal/mol, which is significantly larger than that of the precomplex (13.6 kcal/mol). The calculations show that three reaction channels are open as exothermic reactions in the S_N2 reaction. These channels are expressed by

$$OH^-(H_2O)+CH_3Cl \rightarrow CH_3OH+Cl^-+H_2O \quad \text{(channel I)}$$
$$\rightarrow CH_3OH+Cl^-(H_2O) \quad \text{(channel II)}$$
$$\rightarrow CH_3OH\cdots H_2O+Cl^- \quad \text{(channel III)}.$$

Channel I is "complete (three-body) dissociation channel" in which the product molecules ($CH_3OH+Cl^-+H_2O$) dissociate completely from each other after the reaction. In channel II, the Cl^- ion is solvated by a water molecule which forms a $Cl^-\cdots H_2O$ complex as a product (denoted by "solvation channel"). In channel III, the CH_3OH molecule is solvated by a water molecule. The products are $CH_3OH\cdots H_2O$ and Cl^- (denoted by "complex formation channel"). The reaction energies for channels I, II, and III are calculated to be 21.8, 37.3, and 28.4 kcal/mol, respectively. From the static *ab initio* calculations, it can be suggested that the most favorite channel is the solvation channel (channel II). This is due to the fact that the solvation energy in $Cl^-(H_2O)$ is larger than that in $CH_3OH\cdots H_2O$ (15.5 vs 6.7 kcal/mol, respectively).

It is found that the HF/3-21+G(d) calculation gives a reasonable energetics and shape of the potential energy surface for the reaction system. Hence, direct *ab initio* MD calculation will be carried out at the HF/3-21+G(d) level throughout.

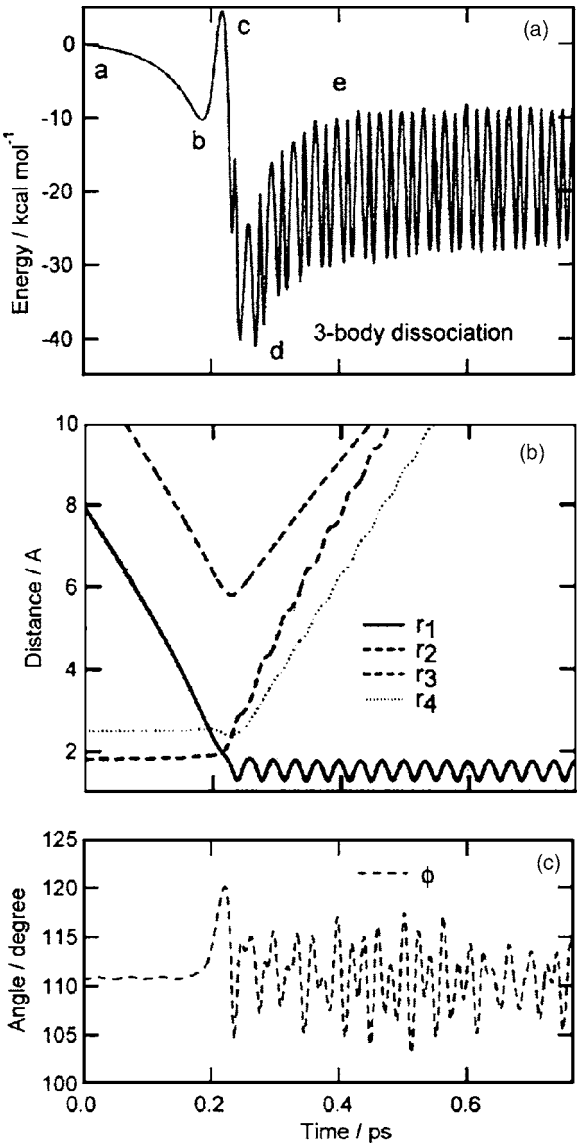

FIG. 4. Potential energy of the system (A), interatomic distances (B), and angles (C) vs reaction time for channel I.

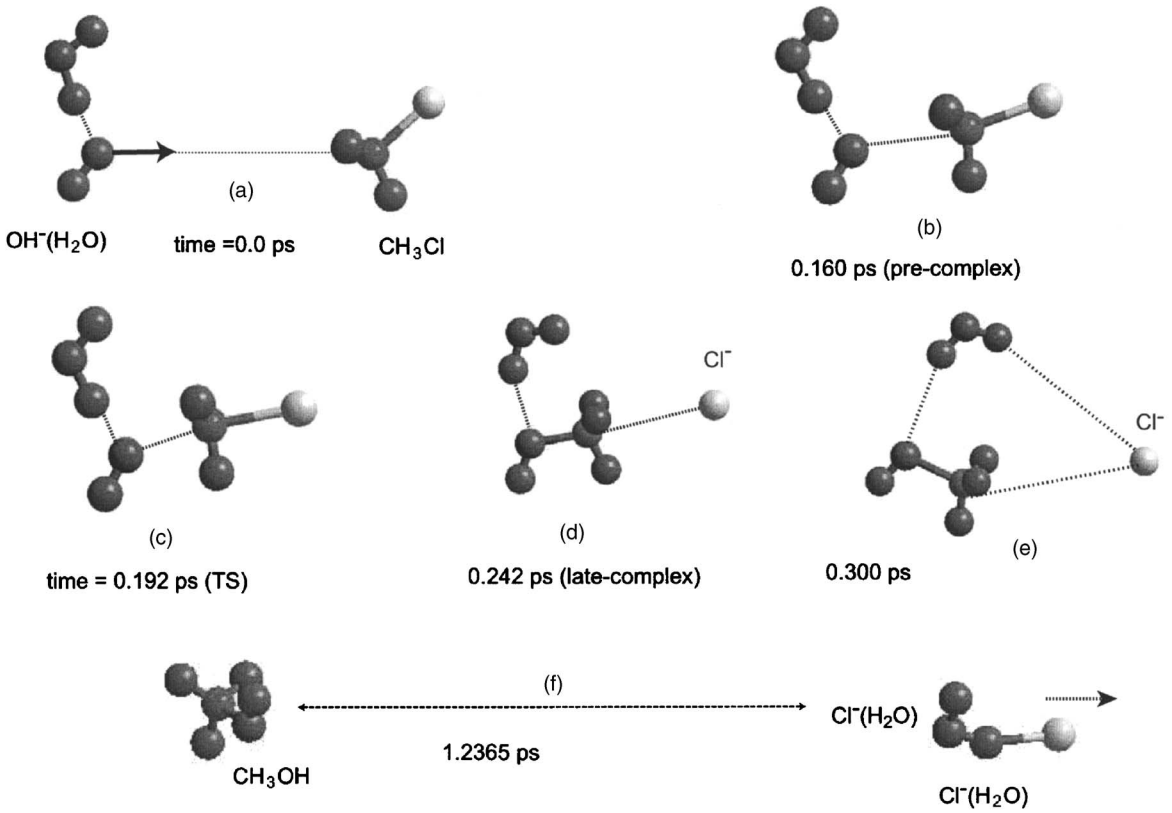

FIG. 5. Snapshots of the conformations for a typical trajectory for channel II illustrated as a function of reaction time.

B. Results of direct *ab initio* MD calculations

A total of 150 trajectories are run from the randomly selected initial configurations between CH_3Cl and $OH^-(H_2O)$. From the trajectory calculations, it is found that three reaction channels, I, II, and II, are concerned with the microsolvated S_N2 reaction $OH^-(H_2O)+CH_3Cl$. In the following sections, we show the profile of typical trajectories for channels I, II, and III and discuss the reaction mechanism.

1. Sample trajectory for channel I

In this section, a profile of a typical trajectory for channel I is discussed. Snapshots of the geometrical configurations are illustrated in Fig. 3. The center-of-mass collision energy is 25.0 kcal/mol. At time zero (point a), $OH^-(H_2O)$ is located at $r_1=7.9731$ Å from CH_3Cl. The OH^- ion is solvated by a water molecule with a hydrogen bond, where one of the protons of H_2O is oriented toward OH^-. The angles α and β at the initial point are 130.9° and 177.4°, respectively. After starting the reaction, $OH^-(H_2O)$ gradually approaches CH_3Cl, and the trajectory enters the region of the precomplex $(H_2O)OH^-\cdots CH_3Cl$. The illustration at time of 0.187 ps (point b) is one of the snapshots near the precomplex. The OH^- ion is located at $r_1=2.759$ Å from CH_3Cl. The trajectory passes near the TS region at 0.21–0.22 ps. At 0.2195 ps (point c), the distances of $HO-CH_3Cl$ and C–Cl are calculated to be $r_1=1.8572$ and $r_2=2.0438$ Å, respectively. The C–Cl bond length of CH_3Cl is significantly elongated at TS (2.0438 Å for TS versus 1.8065 Å for free CH_3Cl). The H–C–H angle of $CH_3Cl(=\phi)$ is calculated to be 119.9° indicating that the CH_3 moiety of CH_3Cl at TS is close to a planar structure.

Around the TS, the Walden inversion takes place at a very short time range, 0.22–0.23 ps, suggesting that this inversion occurs as a very fast process. After the TS, the trajectory passes around the late-complex region at time =0.270 ps (point d). However, the structure of the late complex is different from that obtained by the static *ab initio* calculation: there is no hydrogen bond between Cl^- and CH_3OH in the complex. This result indicates that the trajectory passes by away from the minimum energy point of the precomplex. And then, Cl^- and H_2O leave rapidly from CH_3OH. Finally, the products are completely dissociated from each other $(CH_3OH+Cl^-+H_2O)$, indicating that three-body dissociation takes place after the reaction. The relative velocities of Cl^- and H_2O with respect to CH_3OH are 2862 and 2613 m/s, respectively, in the case of this sample trajectory.

Figure 4(a) shows the PE of the system for channel I plotted as a function of time, while the nuclear distances and angle are plotted in parts B and C, respectively. The zero level of PE corresponds to the potential energy in the initial separation $OH^-(H_2O)+CH_3Cl$ at time zero (point a). After starting the reaction, PE decreases gradually as a function of time, and it reaches an energy minimum at point b (−10.3 kcal/mol at time of 0.187 ps) which corresponds to the precomplex region. The trajectory at the TS region (point c) has an energy maximum of +4.1 kcal/mol. After the TS, it drops suddenly to −41.1 kcal/mol where the trajectory

passes around the late-complex region (point d). The calculations show that pre- and late complexes have very short lifetimes, and it is dissociated rapidly to three product molecules ($CH_3OH+Cl^-+H_2O$).

Time propagations of inter- and intramolecular distances are plotted as a function of time in Fig. 4(b). At time zero, the distance of OH^- from CH_3Cl is $r_1=7.9431$ Å. After starting the reaction, the distance (r_1) decreases gradually, which means that $OH^-(H_2O)$ approaches CH_3Cl. The distances r_2 and r_4 are almost constant up to TS. After TS, these distances increase suddenly, which means that the three-body dissociation, leading to the products ($Cl^-+H_2O+CH_3OH$), occurs after the reaction. The C–OH distance (r_1) vibrates in the range of 1.3–1.6 Å, which means that the C–OH stretching mode of CH_3OH is vibrationally excited after the reaction. The CH_3 umbrella mode of CH_3OH [denoted by ϕ in Fig. 4(c)] vibrates in the range of 105–115°. These results imply that the internal modes of CH_3OH are slightly excited after the reaction.

2. Sample trajectory for channel II

In this section, the reaction dynamics of a sample trajectory for channel II is discussed. Snapshots are illustrated in Fig. 5. This sample trajectory has geometrical parameters with distances $r_1=7.000$ and $r_2=1.807$ Å, and angles $\alpha=111.4°$ and $\beta=41.7°$ at time zero (point a). The center-of-mass collision energy is 15.0 kcal/mol. After starting the reaction, $OH^-(H_2O)$ approaches CH_3Cl and the precomplex is formed at 0.16 ps (point b). The OH^- is located at $r_1=2.6854$ Å from CH_3Cl which is close to the same distance in channel I (2.76 Å). The C–Cl bond is slightly elongated by the complex formation ($r_2=1.8753$ Å). The proton of H_2O is oriented toward the Cl atom of CH_3Cl, but the distance between H_2O and Cl is long at this point ($r_3=5.8196$ Å).

The trajectory reaches the TS at 0.192 ps (point c) where the distance parameters are $r_1=1.9800$, $r_2=2.0015$, and $r_3=5.2096$ Å, and the angle parameters are $\alpha=101.0°$ and $\phi=118.2°$. At 0.242–0.300 ps (points d and e), it is found that the H_2O molecule passes over the methyl group to go along with Cl^-. After that, the water molecule chases the leaving Cl^- ion, and the hydrated Cl^- ion is formed at 1.23 ps. The final product in this trajectory is $Cl^-(H_2O)+CH_3OH$ (point f).

The time propagation of the geometrical parameters and the change of the PE are plotted as functions of time in Fig. 6. After starting the reaction, the PE decreases gradually to −10.5 kcal/mol where the trajectory enters the region of the precomplex (point b). Immediately, the trajectory reaches the transition state (point c). After that, it drops suddenly to −48 kcal/mol (point c). This energy minimum is similar to those of channels I and II. The PE increases with increasing time, but it decreases again. At 0.125 ps, the PE reaches a minimum. This minimum is caused by the solvation of Cl^- by a water molecule. Finally, this trajectory gives $Cl^-(H_2O)+CH_3OH$ (channel II). Time propagation of the bond distance (r_3) corresponds to that of the PE.

The relative translational energy between $Cl^-(H_2O)$ and

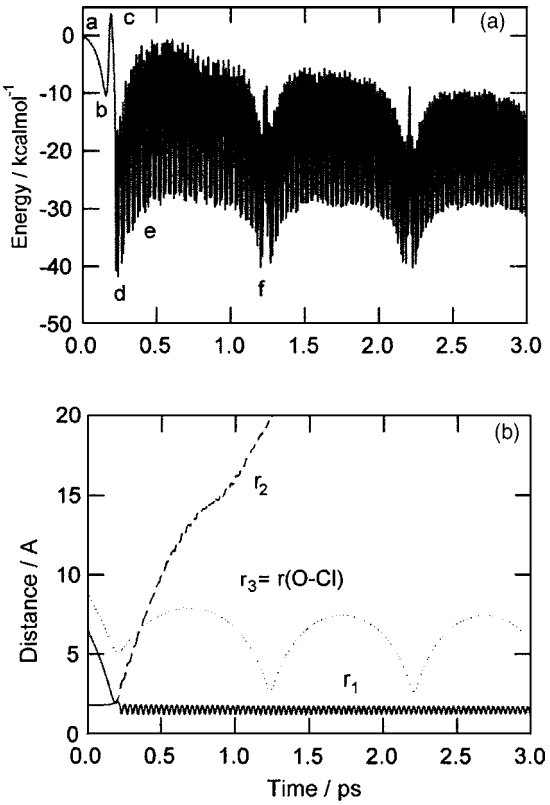

FIG. 6. Potential energy of the system (A), interatomic distances (B), and angles (C) vs reaction time for channel II.

CH_3OH is calculated to be 4.2 kcal/mol in this sample trajectory. This energy is 8% of the total available energy. It should be noted that the intermolecular motion between Cl^- and H_2O vibrates with a time period of 0.975 ps, indicating that $Cl^-(H_2O)$ formed by channel II has a large amplitude motion between Cl^- and H_2O. This is due to the fact that $Cl^-(H_2O)$ is formed by a long-range attractive force between Cl^- and H_2O at a long separation.

3. Sample trajectory for channel III

Snapshots for channel III are illustrated in Fig. 7. This is a typical trajectory for channel III. The collision energy is 25.0 kcal/mol. At initial separation, the angle α is close to collinear ($\alpha=173.5°$) at time zero (point a). The angle is kept at $\alpha=179.9°$ in the precomplex region at time of 0.1475 ps (point b). At the TS, the angle is also kept at $\alpha=179.8°$. After the TS (point c), the water molecule is still bound to CH_3OH by a hydrogen bond and Cl^- leaves rapidly from the complex. Hence, the products in this trajectory are Cl^- and the water-methanol complex. At 0.4065 ps (point e), Cl^- leaves from the $CH_3OH\cdots H_2O$ complex, and it is fully separated. The relative translational energy between Cl^- and $CH_3OH\cdots H_2O$ is calculated to be 20.0 kcal/mol in this sample trajectory, which is 37% of the total available energy.

The time propagation of PE is plotted as a function of time in Fig. 8, the PE is minimized at time of 0.1475 ps (−7.3 kcal/mol at point b). After formation of the precomplex, the trajectory reaches the TS at 0.1910 ps (+6.2 kcal/mol at point c). The PE is minimized again in the late-complex region (−43.9 kcal/mol at point d). Time

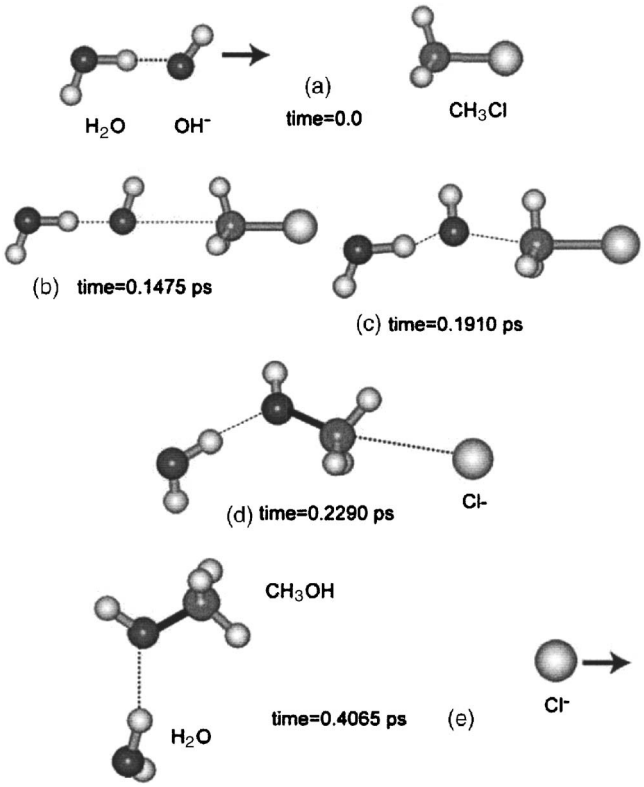

FIG. 7. Snapshots of the conformations for a typical trajectory for channel III illustrated as a function of reaction time.

propagations of inter- and intramolecular distances are plotted as a function of time [Fig. 8(b)]. The distance between H_2O and OH^- is r_4=2.4849 Å at time zero. This distance is kept during the reaction up to the TS. After the TS, the distance vibrations in the range of 2.20–3.60 Å occur. However, the dissociation of H_2O from CH_3OH does not occur after the reaction. Finally, this trajectory gives the products CH_3OH-H_2O and Cl^-.

4. Summary of the trajectory calculations

A total of 50 trajectories were run from the initial configurations selected randomly at each collision energy. From the calculations, it is found that the major reaction channels are channels I and III in the reaction $OH^-(H_2O)+CH_3Cl$. In both channels, only Cl^- is produced as a product ion. Therefore, distinguishing of these channels will be difficult with recent experimental techniques. On the other hand, channel II is minor in all collision energies, although this channel is energetically the most favored of all channels.

The branching ratios for the three channels are plotted in Fig. 9 as a function of collision energy. The branching ratios for channels I and III are drastically changed as a function of collision energy: channel III is dominant at low collision energy (E_{coll}=10 kcal/mol), whereas channel I becomes dominant at higher collision energy (25 kcal/mol). However, the total ratio of the Cl^- formation channels (i.e., channels I plus III) is almost constant, although the total ratio decreases slightly with increasing collision energy. The branching ratio for channel II is small at all collision energies. Thus, the present direct *ab initio* MD calculations suggest that the

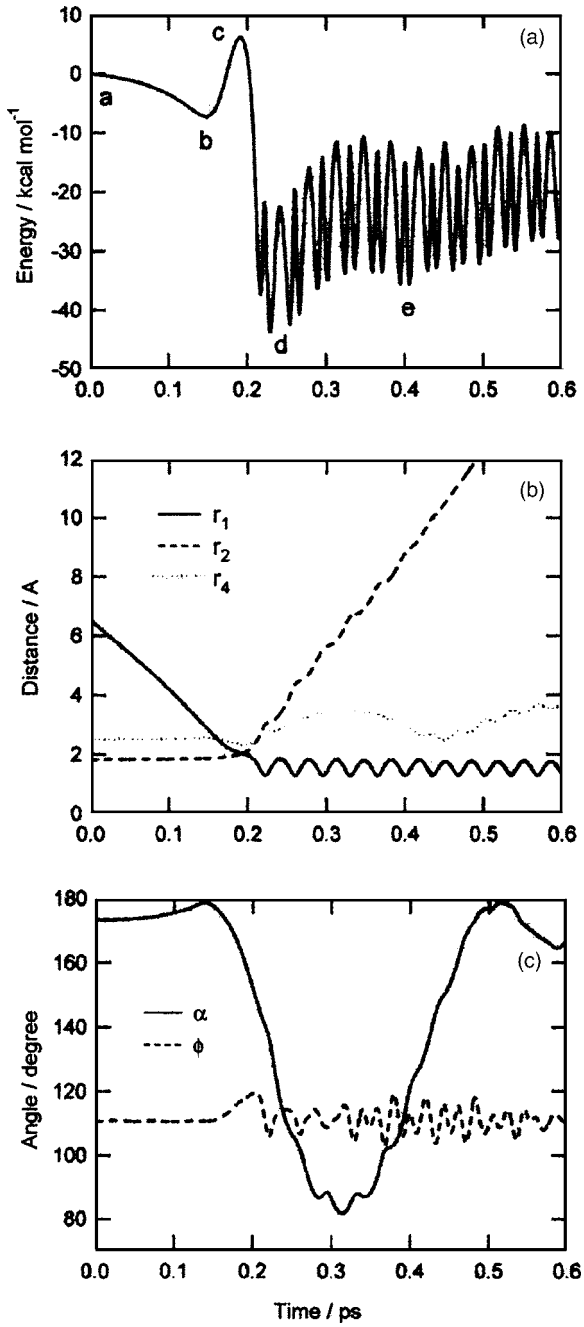

FIG. 8. Potential energy of the system (A), interatomic distances (B), and angles (C) vs reaction time for channel III.

branching ratios of the product channels are drastically changed as a function of collision energy.

Lastly, it should be noted that these results were obtained from studies of a limited number of collision angles (backside attack collisions are only calculated). Therefore, the branching ratios cannot be compared directly with experiment. However, qualitative features obtained in the present calculations may be essentially consistent with experiment.

IV. DISCUSSION

A. Summary of the present study

The present calculations indicate that the reaction probability is greatly affected by only one water molecule. The

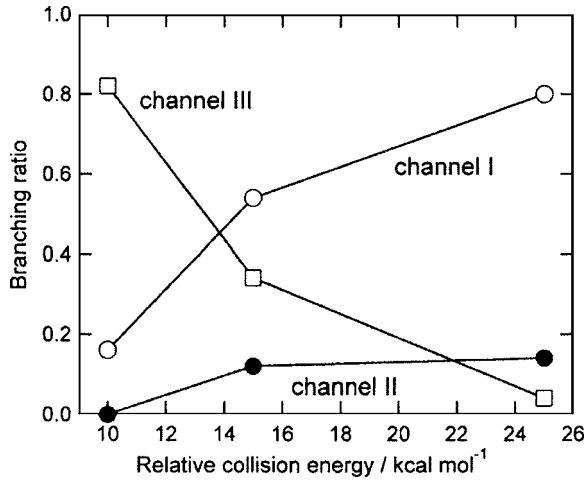

FIG. 9. Branching ratios for three reaction channels I, II, and III calculated by direct *ab initio* MD method. The results are obtained by the trajectory calculations from limited collision angles (backside attack collisions are only calculated).

dynamics calculations showed that the position of H_2O relative to the $OH^-\cdots CH_3Cl$ molecular axis (i.e., angle α) influences strongly the reaction channels and reaction probability. Collisions from the initial configurations with angle $\alpha=80°-180°$ give reactive products, but the collisions from $\alpha<80°$ are nonreactive. Also, the probability is affected by angle b. Hence, the reaction probability in the reaction system $OH^-(H_2O)+CH_3Cl$ is at least two times smaller than that of nonsolvent system OH^-+CH_3Cl.

Figure 10 shows the schematic illustration of populations for three reaction channels as a function of angle (α) and model of collision. The dynamics calculation shows that the major product is Cl^- (channels I and III), although channel II is energetically most favorable in the present reaction. Channel II takes place from a narrow angle region ($\alpha=80°-110°$ and $\beta=20°-40°$). If $OH^-(H_2O)$ approaches CH_3Cl from a collinear position [i.e., the angle of $H_2O\cdots OH^-\cdots CH_3Cl(\alpha)$ is close to 180°], the collision takes place like billiards: the excess energy of $OH^-(H_2O)$ (=translational energy+reaction energy) is efficiently transferred into the translational energy of the Cl^- ion, whereas the energy is hardly transferred to an intermolecular stretching mode between H_2O and CH_3OH. Hence, these collisions give the products ($CH_3OH-H_2O+Cl^-$). This is due to the fact that the mass of $OH^-(H_2O)$ (=36.0 g/mol) is almost equivalent to that of Cl^- (=35.5 kcal/mol). Therefore, the solvation of H_2O to CH_3OH is still remained after the collision (channel III). When $OH^-(H_2O)$ approaches from a perpendicular position (i.e., the angle α is close to 90°), the water molecule slides efficiently from OH^- to Cl^- at the collision. The jump of H_2O gives $Cl^-(H_2O)$ (channel III). In the case of intermediate angles ($\alpha=110-160°$), the excess

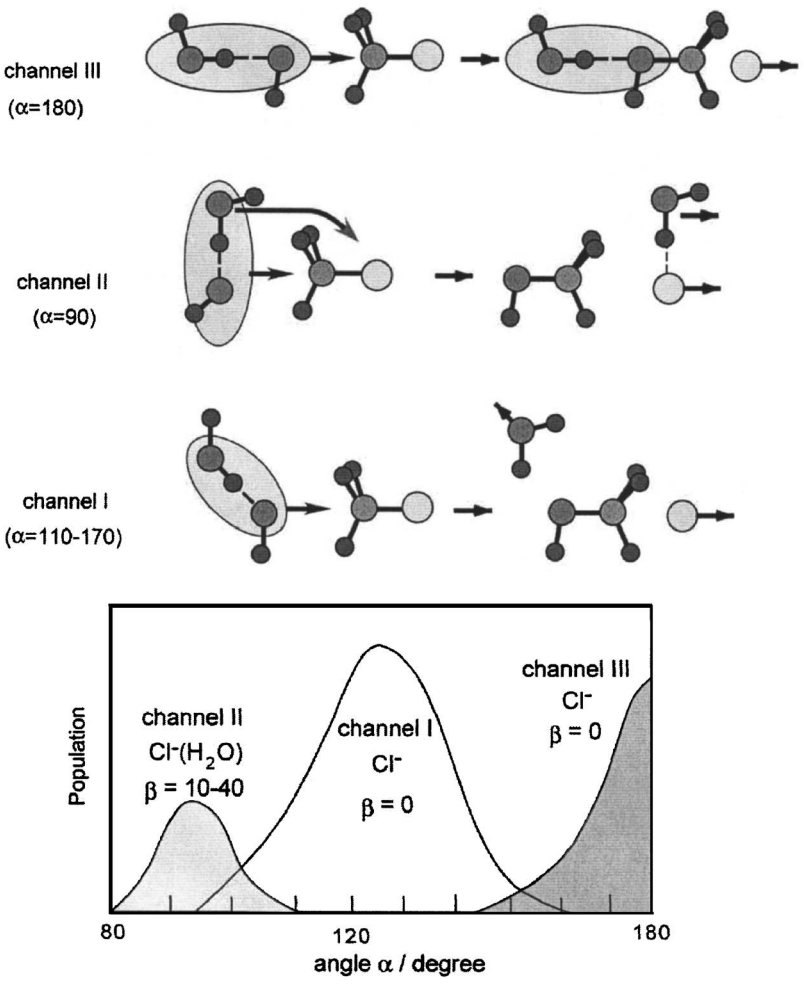

FIG. 10. Schematic illustration of reaction model and populations for the microsolvated S_N2 reaction $OH^-(H_2O)+CH_3Cl$.

energy is efficiently transferred into the translational modes of H_2O and Cl^- (channel II). Hence, three-body dissociation takes place in this angle region (channel I).

B. Comparison with the experiment

Although solvent effects on the S_N2 reaction are important for understanding common organic reactions, the experiments for the microsolvated S_N2 reaction of the type $X^-(H_2O)_n+CH_3Y$ (X,Y=F, Cl, Br, and OH^-) are quite limited. Henchman *et al.*[25] applied a selected ion flow tube (SIFT) at 300 K and a double mass spectrometer relative to a collision energy of 0.3 eV to the S_N2 reaction $OH^-(H_2O)_n+CH_3Br$ (n=0–3). They showed that the reaction rate for n=1 is 65% of that of n=0. The similar value was obtained by flowing afterglow measurements. Viggiano *et al.* investigated the temperature dependence of rate constant and branching ratios of the reaction $OH^-(H_2O)_n+CH_3Br$ (n=0–4).[26] They showed that the reactivity decreases drastically with increasing solvation number (n). For n=1, the rate constant is about a factor of 1.5 smaller than that for the n=0 reaction. Hierl *et al.* measured cross sections and the product distribution for $OH^-(H_2O)_n+CH_3Cl$ (n=0–2) over the relative collision energy range of 0.1–5.0 eV.[22] They found that increasing the hydration number of the reactant ion OH^- (n) decreases the S_N2 reaction probability. Thus, the existence of one water molecule diminishes the reaction rate. The present calculation supports these experimental finding and indicates that the decrease of the reaction rate is caused by a steric hindrance originated by the position of water molecule around OH^-.

For the branching ratio for the reaction channels, Henchman *et al.*[25] showed that the main product channel is Br^- formation in $OH^-(H_2O)+CH_3Br$, whereas the $Br^-(H_2O)$ channel is minor. O'Hair *et al.*[18] also observed that the main product of the reaction is free Cl^- ion, whereas $Cl^-(H_2O)$ is minor in $F^-(H_2O)+CH_3Cl$. Viggiano *et al.* investigated branching ratios of the reaction $OH^-(H_2O)_n+CH_3Br$ (n=1).[26] The reaction products are Br^- (90%) and $Br^-(H_2O)$ (10%). These results are in good agreement with the present calculations. This is due to the fact that collisions from limited angles only give the $Cl^-(H_2O)$ product. Hence, the efficiency of channel II becomes smaller.

Also, the present study predicts that the Cl^- ion is formed via both channels I and III, which are difficult to distinguish experimentally. To confirm this prediction, further experiment to detect the product formed from channel III will be required.

C. Comparison with the previous theoretical works

Re and Morokuma calculated energy diagrams for the reaction $OH^-(H_2O)+CH_3Cl$ at several levels of theory. They suggested that the most favorite channel is the solvation channel (channel II), which has an exothermic energy of 37.3 kcal/mol at the MP2/aug-cc-pVDZ level. The energy level of channel I was 15.5 kcal/mol higher than that of channel II. These features and energetics are in reasonable agreement with the present results, as shown in Fig. 2.

The structures at the TS for the microsolvated S_N2 reactions, $X^-(H_2O)+CH_3Y$, have been calculated by Hu and Truhlar.[19] For a symmetric microsolvated S_N2 reaction of $Cl^-(H_2O)$ with CH_3Cl (i.e., $X=Y$=Cl), the symmetric TS structure with a C_{2v} symmetry was obtained. However, in the case of the asymmetric S_N2 reaction $F^-(H_2O)+CH_3Cl$, the calculated saddle point geometry shows that the water molecule is still hydrogen bonded to the fluorine atom and does not interact with the Cl atom. They failed to find another saddle point that corresponds to the reaction with the water molecule moving in a concerted way from the fluorine atom side to the chloride atom side. Also, they pointed out a nonsynchronous reaction path in which the H_2O molecule is transferred to the Cl^- after the dynamical bottleneck to the reaction. These feature obtained for the reaction $F^-(H_2O)+CH_3Cl$ are similar to the present S_N2 reaction $OH^-(H_2O)+CH_3Cl$. Our dynamics calculations support strongly their prediction.

V. CONCLUDING REMARKS

In the present study, we have introduced several approximations to calculate the potential energy surface and to treat the reaction dynamics. First, we assumed a HF/3-21+G(d) potential energy surface in the *ab initio* MD calculations throughout. As shown in previous papers,[14] the shape of the PES for the OH^-+CH_3Cl reaction system calculated at the HF/3-21+G(d) level of theory is in good agreement with those of QCISD/6-311G(d,p) and MP2/aug-cc-pVDZ levels. Therefore, the level of theory may be effective enough to discuss qualitatively the reaction dynamics for the $OH^-(H_2O)+CH_3Cl$ reaction system. However, a more accurate wave function may provide deeper insight into the dynamics. Second, we calculated 50 trajectories at each collision energy. The number of trajectories may be enough to allow us to discuss the qualitative features of the dynamics, but many more are required to obtain the accurate branching ratio of the reaction channels. Despite several assumptions introduced here, the results enable us to obtain valuable information on the mechanism of the microsolvated S_N2 reaction.

ACKNOWLEDGMENT

The author acknowledges a partial support from a Grant-in-Aid for Scientific Research (C) from the Japan Society for the Promotion of Science (JSPS).

[1] J. K. Laerdahl and E. Uggerud, Int. J. Mass. Spectrom. **214**, 277 (2002), and references therein.
[2] S. M. Villano, S. Kato, and V. M. Bierbaum, J. Am. Chem. Soc. **128**, 736 (2006), and references therein.
[3] A. A. Viggiano and A. J. Midey, J. Phys. Chem. A **104**, 6786 (2000).
[4] C. Hennig, R. B. Oswald, and S. Schmatz, J. Phys. Chem. A **110**, 3071 (2006).
[5] Y. Ren and H. Yamataka, Org. Lett. **8**, 119 (2006).
[6] S. Schmatz, J. Chem. Phys. **122**, 234306 (2005).
[7] J. M. Gonzales, W. D. Allen, and H. F. Schaefer, J. Phys. Chem. A **109**, 10613 (2005).
[8] S. Y. Re and K. Morokuma, Theor. Chem. Acc. **112**, 59 (2004).
[9] S. Y. Yang, P. Fleurat-Lessard, P. I. Hristov, and T. Ziegler, J. Phys. Chem. A **108**, 9461 (2004).

[10] L. P. Sun, E. Y. Chang, K. Y. Song, and W. L. Hase, Can. J. Chem. **82**, 891 (2004).
[11] H. Yamataka, M. Aida, and M. Dupuis, J. Phys. Org. Chem. **16**, 475 (2003).
[12] M. Pagliai, S. Raugei, G. Cardini, and V. Schettino, J. Chem. Phys. **119**, 9063 (2003).
[13] Trajectory studies for the S_N2 reaction by Professor Hase's group: W. L. Hase, Science **266**, 998 (1994); H. Wang and W. L. Hase, Int. J. Mass Spectrom. Ion Process. **167**, 573 (1997); D. J. Mann and W. L. Hase, J. Phys. Chem. A **102**, 6208 (1998); G. Li and W. L. Hase, J. Am. Chem. Soc. **121**, 7124 (1999); L. P. Sun, K. Y. Song, W. L. Hase, M. Sena, and J. A. Riveros, Int. J. Mass. Spectrom. **227**, 315 (2003); Y. F. Wang, W. L. Hase, and H. B. Wang, J. Chem. Phys. **118**, 2688 (2003); H. Wang and W. L. Hase, J. Am. Chem. Soc. **199**, 3093 (1997); S. L. Craig and J. I. Brauman, J. Phys. Chem. A **101**, 4745 (1997).
[14] H. Tachikawa, M. Igarashi, and T. Ishibashi, J. Phys. Chem. A **106**, 10977 (2002); H. Tachikawa and M. Igarashi, Chem. Phys. Lett. **303**, 81 (1999); M. Igarashi and H. Tachikawa, Int. J. Mass. Spectrom. **181**, 151 (1998); H. Tachikawa, Can. J. Chem. **83**, 1597 (2005); H. Tachikawa and M. Igarashi, Chem. Phys. **324**, 639 (2006).
[15] S. L. VanOrden, R. M. Pope, and S. W. Buckner, Org. Mass Spectrom. **26**, 1003 (1991).
[16] S. Kato, J. Hacaloglu, G. E. Davico, C. H. DePuy, and V. M. Bierbaum, J. Phys. Chem. A **108**, 9887 (2004); B. Bogdanov and T. B. McMahon, Int. J. Mass. Spectrom. **241**, 205 (2005); J. V. Seely, R. A. Morris, and A. A. Viggiano, J. Phys. Chem. A **101**, 4598 (1997).
[17] H. van der Wel, N. M. M. Nibbering, J. C. Sheldon, R. N. Hayes, and J. H. Bowie, J. Am. Chem. Soc. **116**, 3609 (1994); A. Gonzalez-Lafont, T. N. Truong, and D. G. Truhlar, J. Phys. Chem. **95**, 4618 (1991); X. G. Zhao, D.-H. Lu, Y.-P. Liu, G. C. Lynch, and D. G. Truhlar, J. Chem. Phys. **97**, 6369 (1992).
[18] R. A. J. O'Hair, G. E. Davico, J. Hacaloglu, T. T. Dang, C. H. DePuy, and V. Bierbaum, J. Am. Chem. Soc. **116**, 3609 (1994).
[19] W.-P. Hu and D. G. Truhlar, J. Am. Chem. Soc. **116**, 7797 (1994).
[20] H. Tachikawa, J. Phys. Chem. **105**, 1260 (2001).
[21] H. Tachikawa, J. Phys. Chem. **104**, 495 (2000).
[22] P. M. Hierl, J. F. Pauloson, and M. J. Henchman, J. Phys. Chem. **99**, 15655 (1995).
[23] S. Y. Re and K. Morokuma, J. Phys. Chem. A **105**, 7185 (2001).
[24] M. J. Frisch, G. W. Trucks, H. B. Schlegel *et al.*, GAUSSIAN 03, Revision B.04, Gaussian, Inc., Pittsburgh, PA, 2003.
[25] M. Henchman, J. F. Paulson, and P. M. Hierl, J. Am. Chem. Soc. **105**, 5509 (1983).
[26] A. A. Viggiano, S. T. Arnold, R. A. Morries, A. F. Ahrens, and H. Hierl, J. Phys. Chem. **100**, 14397 (1996).